

Ultra-Low Power Stationary Plasma Thruster

IEPC-2005-198

*Presented at the 29th International Electric Propulsion Conference, Princeton University,
October 31 – November 4, 2005*

Tsuyohito Ito^{*}, Nicolas Gascon[†], W. Scott Crawford[§], and Mark A. Cappelli[¶]
Stanford University, Stanford, California, 94305-3032, USA

Preliminary results are presented for the operation of a very low power stationary plasma thruster. The thruster design is co-axial, with a 0.5 mm channel width and 4 mm outer channel diameter and is intended to be approximately 1/100 the scale of a typical 1 kW thruster. The magnetic circuit employs a permanent magnet core generating a peak magnetic field of ~ 10 kG. Successful operation is achieved in the 15-40 W power range although at a relatively high mass flow rate (3-5 sccm Xe) – some 5 times that of the design point. This necessity to operate at the high mass flow rate is attributed to the use of a relatively ineffective thoriated tungsten filament cathode source. Despite these initial shortcomings, we have carried out near-field ion energy measurements using a miniaturized retarding potential probe to verify ion production and acceleration. We have also characterized the characteristic “breathing mode” instability which persists during operation in the 160-280V range, and which lies in the 40-70 kHz frequency range.

I. Introduction

Hall discharge plasmas have been used in satellite propulsion since the early 1960s [1, 2]. In a typical co-axial configuration, used primarily to close the electron drift current in the Hall direction, an electrical discharge is sustained within a bounded cylindrical dielectric channel. An anode is located at the base of the channel, and serves also as a source of the propellant. A cathode external to the channel provides an initial source of electrons that migrate towards the anode across the predominantly radial magnetic field, which peaks in the range of 100 – 200 G, near the channel exit. At these magnetic fields, and at the relatively low channel pressure (~ 0.1 Pa), the electrons are highly magnetized, and have a Larmor radius of about 10^{-3} m. While the precise mechanism for electron demagnetization is unknown, it is now widely accepted that the cross-field electron current is somewhat anomalous, varying in strength depending on the location within the channel [3, 4]. The partial confinement of the electrons in the strong magnetic field region gives rise to enhanced ionization due to the increased effective residence time of the electrons. This confinement also serves to concentrate the region of potential drop. Ions created in this confinement region are unaffected by the magnetic field because of their large mass, and are rapidly accelerated out of the channel by this resistive field, and neutralized by additional electrons emitted by the cathode. Very high ionization fractions and ion velocities can be generated with these discharges and, due to their high efficiencies (~ 30-50%) and high specific impulse (1000 – 1500 sec), Hall plasma thrusters in the 200 – 50 kW power range are being evaluated for use on commercial, military and research spacecraft.

^{*} Postdoctoral Scholar, Mechanical Engineering Department, tsuyohito@stanford.edu

[†] Research Associate, Mechanical Engineering Department, nicolas.gascon@stanford.edu

[§] Research Assistant, Mechanical Engineering Department, wsc@stanford.edu

[¶] Professor, Mechanical Engineering Department, cap@stanford.edu

There is increased interest in extending operation of Hall thrusters down into <100 W range, for use on power-limited and smaller satellites. The reduction in operational power is concomitant with a reduction in thruster size. The design of a low power Hall thruster should preserve the ratio of the Larmor radius to channel width (which is typically ~ 1 cm in 1 kW designs), necessitating operation at higher magnetic fields. The reduced Larmor scale increases the cyclotron frequency, allowing operation at higher gas density to preserve the classical Hall Parameter. A geometric scaling based on a reduction in power, P , leads to preserving the thrust density as the channel cross section is reduced by the factor of $1/P^2$, and mass flow rate by $1/P$. It is noteworthy that alternative scaling methodologies can be applied to higher power thrusters which preserve the propellant density within the channel [5], as a reduction in the Larmor radius is not necessitated. The scaling of both co-axial and linear-geometry Hall thrusters to lower powers has been discussed previously in the literature [6, 7].

In this paper, we present preliminary results on the design and operation of a very low power co-axial Hall thruster of the stationary plasma thruster type. The approximate application of scaling laws [7] target operation at 10-20 W for a channel width of 0.5 mm and channel diameter of about 5 mm. The peak magnetic field is about 10 kG. The ability to achieve ideal scaling is constrained by the ability to manufacture the channel and magnetic circuit. The design range for the xenon mass flow is ~ 1 sccm. A schematic illustration of the discharge is shown in Fig. 1. Initial tests of the thruster led to overheating and thermal damage. This was mitigated by water cooling the base of the discharge, and by covering the central pole piece with thick (~ 400 μm) polycrystalline diamond plate. As described below, a filament cathode is used in this design. We believe that the inefficiency of this cathode necessitated operation at a mass flow rate that is ~ 5 times that desired. Despite these initial shortcomings, we have carried out near-field ion energy measurements using a miniaturized retarding potential probe to verify ion production and acceleration. We have also characterized the characteristic “breathing mode” instability which persists during operation in the 160-280V range, and lies in the 40-70 kHz frequency range.

II. Experiment

Test facility

Experiments were all carried out in a test facility consisting of a non-magnetic stainless steel chamber approximately 0.6 m in diameter and 1.2 m in length. The chamber is pumped by a single 55 cm diameter cryopump (CVI-TM500) backed by a ~ 60 l/s mechanical pump. The base pressure of the facility is approximately 10^{-7} Torr, as measured by an ionization gauge, uncorrected for xenon. Thruster testing at xenon flow rates of 3-5 sccm results in chamber background pressures $1-5 \times 10^{-5}$ Torr. Research grade ($>99.995\%$) xenon propellant flow is

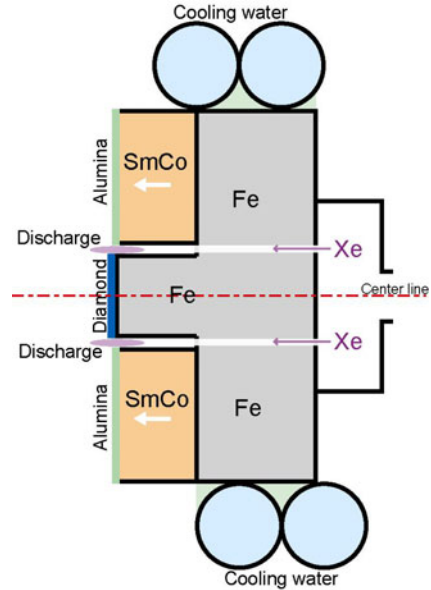


Figure 1. Schematic of low power micro-Hall thruster.

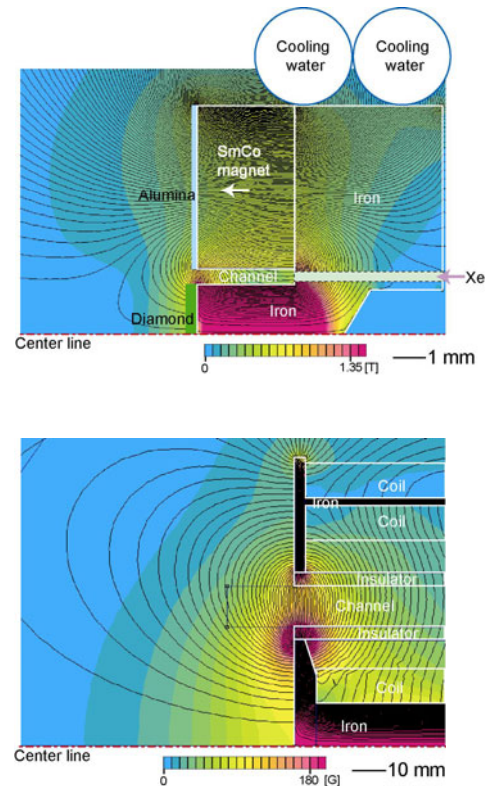


Figure 2. Magnetic field distribution based on simulations using the magnetic structure: (top) Micro hall thruster; (bottom) Stanford Hall thruster.

delivered to the thruster using a 5 sccm mass flow controller (Unit instruments, UFC-1201A).

Micro Hall Thruster

As illustrated in Fig. 1, the magnetic circuit incorporates a ring-type SmCo permanent magnet in conjunction with a high purity iron circuit, and is capable of generating a magnetic field (mostly radial) ranging from 0.5 – 1 Tesla in strength, in the vicinity of the channel exit. The outer diameter of the magnet is 14 mm, the inner diameter is 4 mm, and the thickness is 3 mm. The outer diameter of the channel is 4 mm, the inner diameter is 3 mm – also the outer diameter of the iron core. The magnetic field is not verified experimentally. Instead, we rely on predictions for the precise configuration carried out using a commercially-available finite element solver [8]. The computed magnetic field contours are shown in the top frame of Fig. 2. For comparison, we provide the computed contours for our higher power (90 mm outer diameter) thruster, in the bottom frame of Fig. 2. While both the microthruster and the higher power thruster generate predominantly radial components to the magnetic field near the channel exit, it is apparent that the simplified magnetic circuit associated with the micro-Hall thruster establishes a separatrix at a downstream location of about one channel diameter. This leads to a strong (divergent) lensing effect, which is now believed to be partly responsible for the divergence seen in the ion energy, as discussed below. This unusual field configuration could be corrected by the placement of a trim coil at the base of the thruster. However, it seems that the magnetic flux within the central iron pole piece is already near saturation.

It is noteworthy that unlike traditional stationary plasma thrusters, the channel of this thruster is predominantly metal, at anode potential. As a result, the discharge is highly obstructed, with the anode located essentially near the region of strong magnetic field. We are currently redesigning the thruster to have a ceramic layer on the outer most region of the thruster. The depth of the channel is about 3 mm. Propellant is injected through eight small holes, 0.33 mm in diameter, machined into the iron pole piece.

The anode of the discharge is powered by a Sorensen SCR600-1.7 laboratory power supply capable of providing 600 V and 1.7 A. The anode also has a 4 Ω resistor in series with it to provide a means of monitoring anode current oscillations. Oscillations were recorded as a time-varying voltage drop across this resistor, as measured with a high voltage differential probe (Tektronix PS200) and a 100 MHz digital oscilloscope (Tektronix TDS3014). The cathode used for most of the results presented here is a 1% thoriated tungsten wire, 150 μm in diameter, hand wound to produce a 15 turn spiral filament approximately 1 cm long. It was positioned approximately 7 mm off axis and 9 mm downstream of the exit of the discharge. The filament was powered by a (DC) power supply providing a total current of 14-17 A at a voltage of 2-3 V, dissipating $\sim 40\text{W}$ during thruster operation.

Retarding Potential Analyzer

A retarding potential analyzer (RPA) has been fabricated and employed for measuring the ion energy distribution in low power plasma thrusters. The design used here is a scaled version of that used by Hofer [9]. Figures 3 and 4 show a schematic and photograph of the RPA, respectively. Not shown in the photograph is a graphite shield that surrounds the phenolic body. The diameter of the open aperture is 4 mm. The RPA is of a four-grid design, and each grid has a 38% open area. During operation, both the graphite shield and first grid (Grid 1) are floating providing a minimally-perturbing interface between the analyzer and the plasma. Grid 2 is an electron repelling grid with negative potential that is set to a voltage as high as -25 V , to prevent electrons from entering the ion retarding

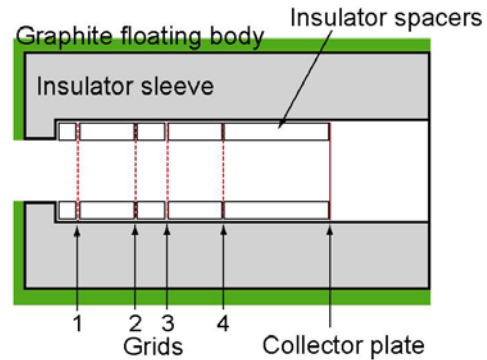


Figure 3. Schematic of retarding potential analyzer.



Figure 4. Photograph of miniaturized retarding potential analyzer (taken before the graphite shield is added). The total probe diameter is 15 mm. The front aperture is 4 mm in diameter.

stage. Grid 3, the ion retarding grid, was swept from 0 to 280V relative to ground potential. Grid 4 is designed as an electron suppressor, which reflects secondary electrons emitted by the collector back to the collector plate. The activation of this suppressor grid can cause a loss in signal, and for the preliminary results shown below, the RPA was operated with this grid tied to the collector potential. Secondary electron emission was minimized by coating the collector plate with a conductive graphite paste. The sum of both the current collected on Grid 4 and the collector plate was measured using a picoammeter (Keithley 485).

The RPA unit was mounted on a computer-controlled rotational stage and an off-axis angle (with the center of the thruster exit plane as the rotational axis) can be selected by remote stepper motor control.

III. Results and Discussion

The thruster described was run at near-design conditions, in voltage limited mode. During operation, the discharge appeared to be fairly uniform around the co-axial channel although on camera, the luminous emission was dominated by the thermal emission from the filament, as seen from the photograph of the discharge during operation, in Fig. 5 below. The $V-I$ characteristics, which are illustrated in Fig. 6, are somewhat typical of Hall discharges, although a clear current saturation branch is never really seen, except perhaps at very high discharge voltages. Discharge stability precluded operation below about 3 sccm. This was attributed to the inefficiency of the cathode. We believe that a more efficient



Figure 5. Photograph of the low power micro-Hall thruster. Note: outer diameter of the channel is 4 mm. A filament locates out of the left edge of this figure.

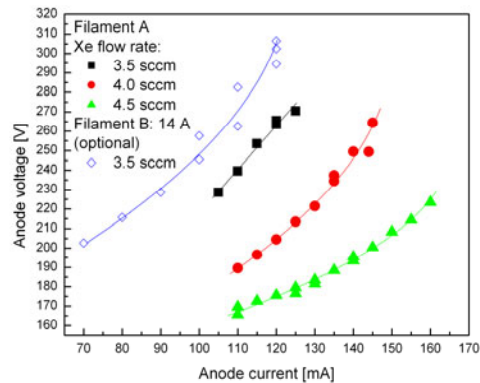


Figure 6. Discharge voltage-current characteristics of the micro Hall thruster. Note: Filament A is the thoriated tungsten filament. Filament B is a ribbon type tungsten filament (General Electric 18A/T10/1-6V).

cathode would permit operation at a lower mass flow rate, closer to design conditions. For example, replacing the thoriated tungsten filament by a (non-thoriated) ribbon type tungsten filament (General Electric 18A/T10/1-6V) greatly reduced the discharge current while at a relatively high flow rate, as expected. Increasing the current through this filament was found to result in an increased anode current, as shown in Fig. 7. However, melting of the filament precluded reaching the level of current needed to operate the discharge below 3 sccm.

We noticed that the performance of the thoriated tungsten filament slowly changed during thruster operation. After extended operation, adjustments and possible replacement of the filaments was necessary. We established a reference discharge condition (120mA-205V with 4 sccm Xe) for benchmarking and adjusting the filament performance. Filament adjustments were made to reproduce this benchmark operating performance. At this operating condition, the mean oscillation frequency in the current was generally reproduced to within 5 % over the range of time needed to obtain complete I-V curves.

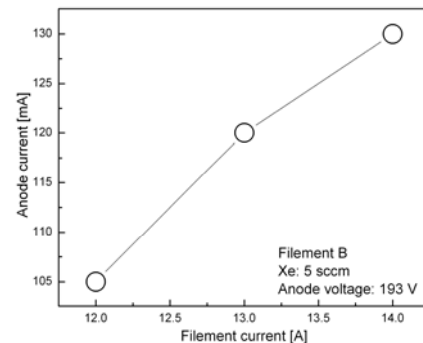


Figure 7. Example of anode current changes due to a filament current: Filament B used is a ribbon type tungsten filament (General Electric 18A/T10/1-6V).

At all conditions investigated, the discharge current exhibited strong oscillations, typical of Hall thrusters – associated with the so-called “breathing mode” instability. This instability is attributed to a disruption in the balance in maintaining propellant within the channel to facilitate current flow to the anode. This balance is established between the introduction and transport of neutral propellant from the anode, and the loss of neutral xenon to ionization and subsequent rapid depletion of the channel of ions as a result of acceleration. The oscillation frequency is expected to scale inversely with the length of the ionization zone, which should be considerably shorter in this thruster due to the operation at higher propellant density. In a typical ~kW scale thruster, this instability is seen at 10-20 kHz. It was anticipated that this discharge would experience this instability at much higher frequencies. Figure 8 shows oscillograms of the discharge current for a range of discharge voltages. Figure 9 gives the results of a spectral analysis of these oscillograms. It is apparent that the disturbances are characterized by sharp fundamental modes in the range of 40 – 80 kHz, with less intense harmonics. Although these frequencies are amongst the highest seen for low power thrusters, they are still lower than expected based on the $1/20^{\text{th}}$ scale of this thruster. We suspect that the relatively low frequency is due to a relatively thick ionization layer. This conjecture would be supported by a relatively broad ion energy distribution, and was the impetus for implementing the RPA studies described below. The frequency of the fundamental component is seen to vary nearly linearly with discharge voltage, as illustrated in Fig. 10. There was only a slight dependence of this frequency on mass flow rate (hence gas density) over the limited mass flow rate range investigated.

The unprocessed RPA signal and extracted ion energy distribution taken 7.5 cm from the exit plane of the thruster operating at a discharge voltage of 221V and mass flow rate of 4 sccm are shown in Figs. 11 and 12, respectively. As expected on the basis of the relatively low breathing mode frequency (indicative of a relatively broad acceleration zone), the measured ion energy distribution is broader in comparison to those seen in larger thrusters [9]. The distributions are clearly non-Gaussian, with a sharp drop in the distribution at high energy, and a persistent low energy tail. The peak in the distribution at 175V is consistent with an approximately 45V plume and cathode fall loss for a discharge voltage of 221V. It is noteworthy that preliminary measurements made at larger angles result in a stronger signal (higher ion current). Also the signals are not symmetric (not shown) about the discharge centerline, likely due to

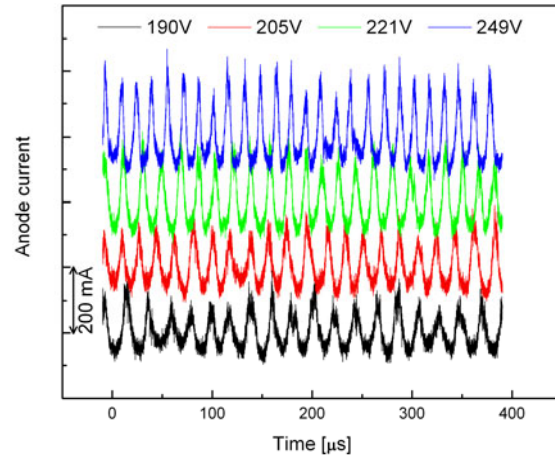


Figure 8. Oscillograms of discharge current.

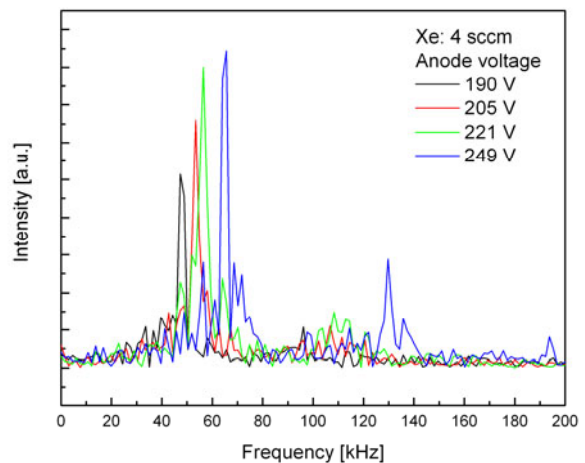


Figure 9. Low frequency spectral analysis of the discharge current.

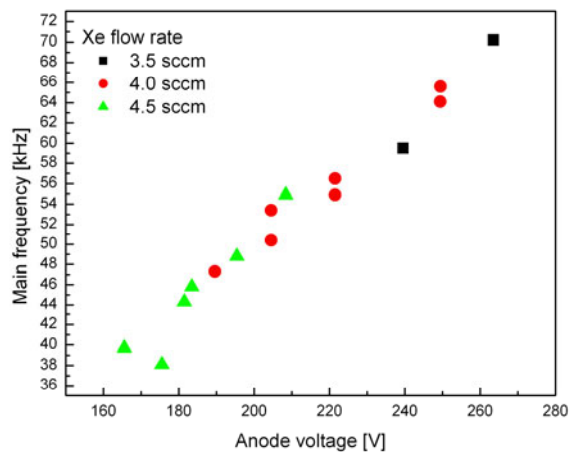


Figure 10. Mean fundamental “breathing mode” frequency as a function of the discharge voltage.

the asymmetric placement of the cathode. The reasons for this off-axis peak at such a large downstream location is not clear, although we speculate that it is partly due to the non-ideal magnetic field distribution shown in Fig. 2 (a), and quite possibly due to the poor filament performance. Angular measurements of the total ion current and ion energy distributions will be studied in more detail in future experiments, where comparisons will be made to thruster operation on a low-power hollow cathode neutralizer. Future measurements are also planned for measuring overall performance such as thrust efficiency and specific impulse.

IV. Conclusion

Preliminary results have been presented for the operation of a very low power stationary plasma thruster. The thruster design is co-axial, with a 0.5 mm channel width and 4 mm outer channel diameter and is intended to be approximately 1/100 the scale of a typical 1 kW thruster. The magnetic circuit employs a permanent magnet core generating a peak magnetic field of ~ 10 kG. Successful operation is achieved in the 15-40 W power range although at a relatively high mass flow rate (3-5 sccm Xe) – some 5 times the design point. This necessity to operate at the high mass flow rate is attributed to the use of a relatively ineffective cathode source. For the most studies presented here, we have employed a thoriated tungsten filament. Despite these initial shortcomings, we have carried out near-field ion energy measurements using a miniaturized retarding potential probe to verify ion production and acceleration. We have also characterized the characteristic “breathing mode” instability which persists during operation in the 160-280V range, and lies in the 40-70 kHz frequency range.

Micro hall thruster operation using a low-flow rate hollow cathode discharge is now in progress. A cathode has strong effect on discharge characteristics as shown in this paper. The operation with the hollow cathode, which has much longer lifetime and hopefully better reproducibility, might be more ideal for understanding the cathode effect. The insulator wall effect on the channel is also under a consideration.

Acknowledgments

This research was supported by a grant from the Air Force Office of Scientific Research with Dr. Mitat Birkan as program manager. The authors would like to thank Mr. Michael Bachand for the design and fabrication of the RPA. Partial support for T. Ito was provided by the JSPS Postdoctoral Fellowships for Research Abroad program.

References

- ¹Brown, C. O., and Pinsley, E. A., “Further Experimental Investigations of a Cesium Hall-Current Accelerator”, *AIAA J.*, Vol. 3, 1965, pp. 853-859.

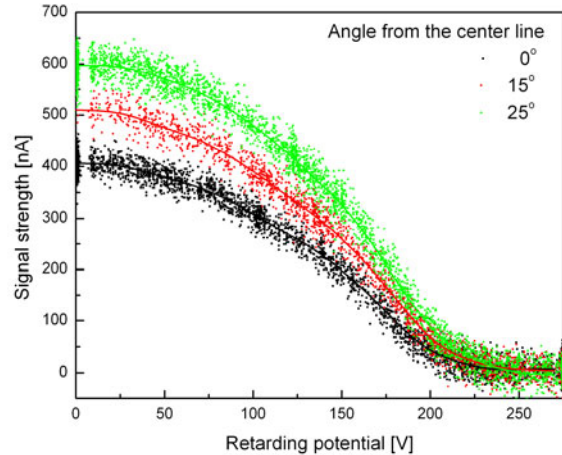


Figure 11. Signal-retarding potential curve of RPA.

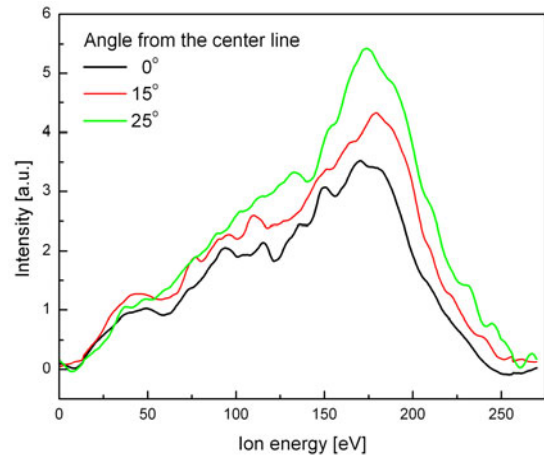


Figure 12. Analyzed ion energy distributions from RPA signals.

²Janes, G. S., and Lowder, R. S., “Anomalous Electron Diffusion and Ion Acceleration in a Low-Density Plasma”, *Phys. Fluids.*, Vol. 9, 1966, pp. 1115-1123.

³Meezan, N. B., Hargus, W. A. Jr., and Cappelli, M. A., “Anomalous electron mobility in a coaxial Hall discharge plasma”, *Physical Review E*, Vol. 63, 2001, 026410.

⁴Fife, J. M., “Hybrid-PIC Modeling and Electrostatic Probe Survey of Hall Thruster”, PhD Thesis, MIT, Cambridge, MA, 1998.

⁵Manzella, D. H., “Scaling Hall Thruster to High Power” PhD Thesis, Stanford University, Stanford, CA, 2005.

⁶Khayms, V., and Martinez-Sanchez, M., “Design of a miniaturized Hall thruster for microsattellites”, *32nd Joint Propulsion Conference*, Lake Buena Vista, FL, 1996, AIAA-96-3291.

⁷Schmidt, D. P., Meezan, N. B., Hargus, W. A. Jr., and Cappelli, M. A., “A low-power, linear-geometry Hall plasma source with an open electron-drift”, *Plasma Sources Sci. Technol.*, Vol. 9, 2000, pp. 68-76.

⁸Meeker D. C., Finite Element Method Magnetics, Version 3.4.1, <http://femm.foster-miller.net>.

⁹Hofer, R., Haas, J., Gallimore, A., “Ion voltage diagnostics in the far-field plume of a high-specific impulse Hall thruster”, *39th Joint Propulsion Conference*, Huntsville, AL, 2003, AIAA-2003-4556.